Increase in chaotic motions of atoms in a large-scale self-organized motion

Tadashi Watanabe and Hideo Kaburaki
Research and Development Group for Numerical Experiments, Japan Atomic Energy Research Institute, Tokai-mura, Naka-gun, Ibaraki-ken, 319-11, Japan
(Received 20 December 1995)

The macroscopic flow transition between heat conduction and convection in the two-dimensional Rayleigh-Bénard system is simulated using the molecular-dynamics method. The heat conduction state, in which motions of atoms are random and a large-scale flow does not appear, is established when the temperature difference between the top and bottom walls is small. It is shown, when the temperature difference is large, that macroscopic convection rolls appear and the trajectories of atoms are along the rolls. The degree of the chaotic motions of atoms is observed in terms of the Lyapunov exponent. In the heat conduction state, the Lyapunov exponent is shown to increase with the average temperature and the temperature difference. It is found that the Lyapunov exponent depends not only on the temperatures but also on the macroscopic flow velocity when the flow field shows the convecting state. The chaotic motions of atoms are shown to increase in the large-scale self-organized motion. [S1063-651X(96)06508-7]

PACS number(s): 47.20.Bp, 47.27.Te, 05.45.+b, 05.70.Ln

I. INTRODUCTION

The Rayleigh-Bénard (RB) system, in which a fluid is contained between two horizontal parallel walls and the bottom wall is kept at a higher temperature than the top wall, is one of the representative nonequilibrium hydrodynamic systems. In the RB system, a heat conduction state is established when the temperature difference between the top and bottom walls is smaller than a critical value, while convection rolls appear due to gravitational forces when the temperature difference exceeds the critical value.

Convection in the RB system has been extensively studied both experimentally and numerically. These studies were reviewed by Ahlers [1] and Cross and Hohenberg [2]. In recent years, RB convection has been studied at the molecular level using the direct simulation Monte Carlo (DSMC) method and the molecular-dynamics (MD) method in order to study the microscopic origin of the macroscopic flow phenomena. The convection rolls were simulated using the DSMC method by Garcia [3] and Stefanov and Cercignani [4]. Garcia and Penland [5] compared velocity distributions in the convection rolls with the numerical solution of the Navier-Stokes equations. The transition between conduction and convection was shown by Watanabe, Kaburaki, and Yokokawa using the DSMC method [6]. The spatial correlations of temperature fluctuations were shown to grow in the transition between heat conduction and convection [7]. The DSMC method has also been applied to the simulation of various types of macroscopic flow phenomena as well as RB convection [8]. The RB convection was also simulated using the MD method by Mareschal and Kestemont [9,10] and Rapaport [11]. Mareschal *et al.* [12], Puhl, Mansour, and Mareschal [13], and Given and Clementi [14] compared the field variables in the convection rolls obtained by the MD method with the results by the hydrodynamic calculations. Although the macroscopic flow phenomena in the RB system were simulated in these studies qualitatively and quantitatively using the particle simulation technique, the microscopic motions of atoms or molecules in the macroscopic flow fields were not discussed. Posch, Hoover, and Kum studied the RB problem using the smooth-particle applied mechanics (SPAM), which is a grid-free particle method for solving the partial differential equations of fluid or solid mechanics [15,16]. The good agreement between the smooth-particle and the Navier-Stokes results was obtained and SPAM was shown to be an interesting bridge between continuum mechanics and molecular dynamics [17].

Besides the RB convection, the MD method has been applied to various types of macroscopic flow problems. Meiburg [18] simulated the vortex shedding past an inclined flat plate. The flow past a circular obstacle was simulated by Rapaport and Clementi [19] and Rapaport [20]. A channel flow was simulated by Hannon, Lie, and Clementi [21] and the MD results were compared with analytical results. The simulation of shock waves in fluids was performed by Holian [22]. The slip length in dilute gases was studied by Bhattacharya and Lie [23,24] and Morris, Hannon, and Garcia [25]. It was shown that not only the RB convection but also various macroscopic flow phenomena could be simulated qualitatively and quantitatively using the MD method. Koplik, Banavar, and Willemsen [26,27] simulated the contact line separating two immiscible fluids. The molecular structure of a wall was taken into account and the no-slip condition of a macroscopic flow at the wall was discussed. Fluid interfaces and free surfaces were studied by Koplik and Banavar [28,29]. The microscopic motions and trajectories of atoms were discussed in these MD studies as well as the macroscopic flow phenomena. The microscopic flow structure of the transition between heat conduction and convection, however, was not studied.

In order to study irreversible nonequilibrium steady states, microscopic flow structures were studied using the MD method. A shear flow at constant internal energy was simulated by Evans [30] and a heat flow with the two boundary regions thermostatted at different temperatures was discussed by Holian, Hoover and Posch [31] and Hoover [32]. The full spectra of Lyapunov exponents for particle systems under an external force field were measured by Posch and Hoover

 © 1996 The American Physical Society

[33]. Posch and Hoover [34] also studied Lyapunov spectra for two- and three-dimensional fluids and solids. The size dependence of Lyapunov spectra was discussed by Hoover and Posch [35,36]. Although macroscopic irreversible nonequilibrium flows with reversible equations of motion were studied in these studies, the macroscopic flow transition or instability was not discussed.

In this paper, the MD method is applied to simulate the macroscopic flow transition between heat conduction and convection in the two-dimensional RB system. It is shown that one nonequilibrium steady state (heat conduction) is obtained when the temperature difference between the top and bottom walls is small, while the other nonequilibrium steady state (convection) appears when the temperature difference is large. In order to study the relationship between the macroscopic flow fields and the microscopic motions of atoms, the degree of the chaotic motions of atoms is discussed in terms of the Lyapunov exponent, which is obtained from the growth rate of the separation distance between two trajectories in the phase space. It is found that the chaotic motions of atoms are increased in the macroscopic convecting state, which is a large-scale self-organized ordered motion of atoms.

II. MD SIMULATION OF THE RAYLEIGH-BÉNARD SYSTEM

The RB conduction-convection system is simulated using the MD method. In this method, the motions of atoms or molecules are simulated by integrating Newton's equations of motion

$$\frac{d^2\mathbf{r}_i}{dt^2}=\frac{\mathbf{F}_i}{m_i},\quad i=1,2,\ldots,N, \tag{1}$$

where $\mathbf{r}_i$ and m_i are the spatial position and the mass of ith particle, respectively, $\mathbf{F}_i$ is the force acting on ith particle, and N is the number of particles in the simulation region. Each pair of particles is assumed to interact through a Lennard-Jones potential

$$\phi_{\mathrm{LJ}}(0<r<3.0\sigma)=4\varepsilon_{\mathrm{LJ}}\left\{\left(\frac{\sigma}{r}\right)^{12}-\left(\frac{\sigma}{r}\right)^{6}\right\}, \tag{2}$$

where the parameters $\varepsilon_{\mathrm{LJ}}$ and σ provide the scales of energy and distance, respectively, and r is the distance between two particles. The force acting on ith particle is the sum of forces from other particles

$$\mathbf{F}_i=-\sum_{j=1}^{N}\nabla_i\phi_{\mathrm{LJ}}(r_{ij}),\quad j\neq i. \tag{3}$$

We assume argon atoms for simulation particles: $m=6.63\times10^{-26}$ kg, $\sigma=3.4\times10^{-10}$ m, and $\varepsilon_{\mathrm{LJ}}/k_B=120$ K, where k_B is the Boltzmann constant. The number of simulation particles is 7200.

The simulation region is a two-dimensional rectangle, which is 6.48×10^{-8} m in width and 3.21×10^{-8} m in height, with an aspect ratio of about 2. The onset of convection for the RB system is predicted from the linear stability analysis of the macroscopic hydrodynamic equations based on the Boussinesq approximation [37]. The wavelength of the perturbation at the onset of convection is about 2 and thus the aspect ratio of the simulation region is set equal to this value [6]. The simulation particles are equally spaced in horizontal and vertical directions initially. The temperature of the top wall is kept constant at 120 K throughout the simulation and that of the bottom wall is also a constant, but ranges from 120 to 600 K. The initial temperature distribution is linear from the bottom to the top wall and the velocity components of the particles are sampled from the Maxwellian distribution corresponding to the temperature. The basic equations (1)–(3) are nondimensionalized using m, $\varepsilon_{\mathrm{LJ}}$, and σ and numerically integrated by the second-order Verlet method [38]. Th time unit characterizing particle motions is $\tau=\{(m\sigma^2)/(48\varepsilon_{\mathrm{LJ}})\}^{1/2}=3.1\times10^{-13}$ sec and the simulation time step is set equal to 0.05τ. The simulation region is divided into 40×20 sampling cells, in which macroscopic flow variables such as flow velocities are calculated. A flow field is obtained by an average of samples during a simulation period of 2000τ (40 000 simulation time steps).

For simplicity, the microscopic structure of the wall surrounding the simulation region is not simulated. The diffuse reflection boundary condition, in which a reflected particle has velocity components randomly sampled from the Maxwellian distribution corresponding to the surface temperature, is assumed at the top and bottom walls. The specular reflection boundary condition, in which the perpendicular velocity component of the incident particle is reversed and the tangential velocity component is unchanged, is assumed at the sidewalls. The gravitational acceleration is chosen to be a hypothetical value so as to minimize density variations [15]:

$$g=\frac{k_B\Delta T}{mL_y}, \tag{4}$$

where ΔT and L_y are the temperature difference and the distance between the top and bottom walls, respectively. The gravitational acceleration given by Eq. (4) is also obtained from the energy balance so that the average increase in kinetic energy of a particle at the bottom wall is sufficient to bring it to the top of the system [9,14]. The gravitational acceleration is added to the right-hand side of Eq. (1).

III. MACROSCOPIC FLOW FIELD

In this section the macroscopic flow filed obtained by the MD method is discussed. Typical transient flow fields are shown in Fig. 1 for a convection state. The bottom wall temperature is 600 K in this case. The velocity fields are in the left column and the corresponding temperature fields are in the right. The velocity and temperature fields in the top row are the average flow fields during the first 2000τ period (from 1 to 40 000 time steps), those in the second row are obtained during the second 2000τ period (from 40 001 to 80 000 time steps), and so on. It is seen in the velocity fields that relatively large flows appear first at around the midelevation. This is also shown in the transient flow fields obtained by the DSMC method [6].

One of the important parameters characterizing the RB system is the Rayleigh number [37], which is defined by

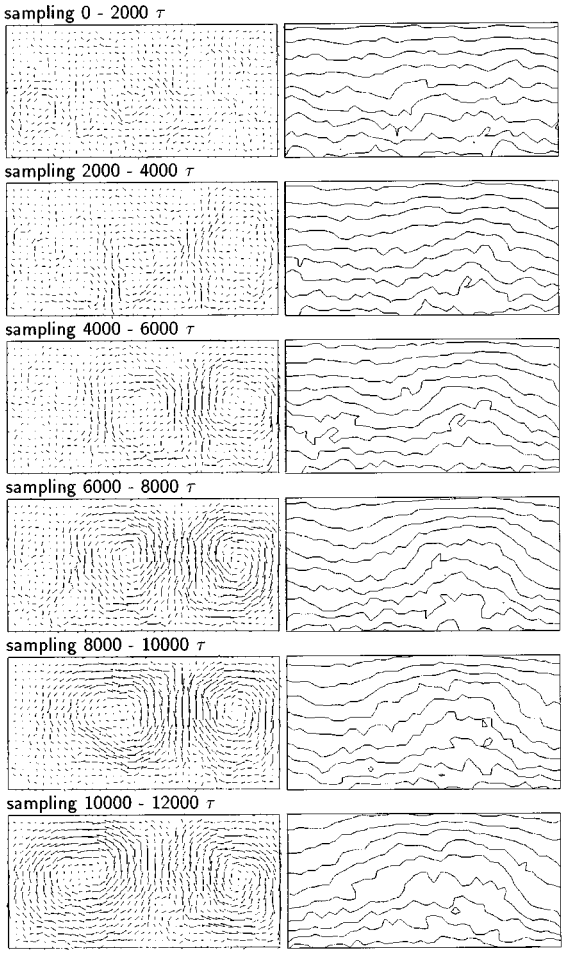

FIG. 1. Typical transient flow fields for a convective state. The bottom wall temperature is 600 K. Velocity and temperature fields obtained by sampling during the 2000τ period (40 000 time steps) are in the left and right columns, respectively.

$$R=\frac{\alpha\Delta T g L_y^3}{\nu\kappa}, \tag{5}$$

where α, ν, and κ are the volume expansion coefficient, the kinematic viscosity, and the thermal diffusivity, respectively. It is well known in the RB system that convection rolls appear when the Rayleigh number exceeds a critical value. For a dense gas, the transport coefficients are given as a function of the density and temperature [39,40] and the Rayleigh number is obtained by

$$R=R'(\rho^*)L_y^2\left(\frac{\Delta T}{T^*}\right)^2, \tag{6}$$

based on the Enskog theory, where ρ^* and T^* are the average density and temperature in the system, respectively, and $R'(\rho^*)$ is the density-dependent part of the Rayleigh number.

After stable flow fields are established, the maximum flow velocity is shown in Fig. 2 against a parameter ε, which is defined by

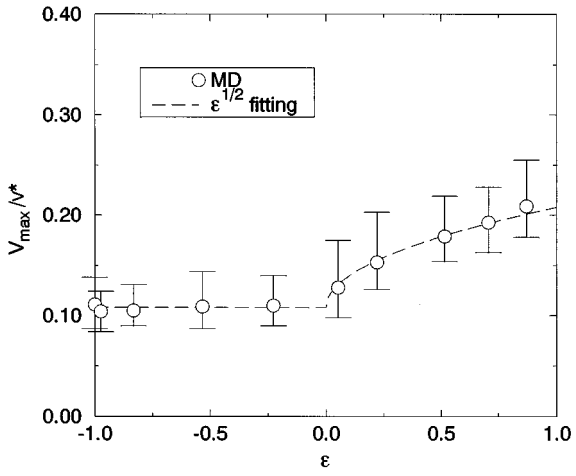

FIG. 2. Maximum flow velocity vs the parameter $\varepsilon=(R-R_c)/R_c$, where the critical Rayleigh number (R_c) is determined from a fit of $\varepsilon^{1/2}$. The data points (○) show a long-time average in the steady state and the error bars indicate the range of data distributions.

$$\varepsilon=\frac{R-R_c}{R_c}, \tag{7}$$

where R_c is the critical Rayleigh number. The critical Rayleigh number is defined above which convection states appear and is obtained at $(\Delta T/T^*)^2=0.95$ in our simulation. The theoretical value of the critical Rayleigh number for our system is about 1708 from the linear stability analysis [37] and the value of $(\Delta T/T^*)^2$ corresponding to the theoretical critical Rayleigh number is calculated to be about 1.17 from Eq. (6) for our simulation conditions. As the simple boundary conditions are used in our simulation, the observed value of $(\Delta T/T^*)^2=0.95$ is used in the following so that the onset of convection corresponds to $\varepsilon=0$.

In Fig. 2 the maximum flow velocity $V_{\max}$ is normalized by the reference velocity defined as the average thermal speed for the average temperature in the system $v^*=(8k_BT^*)^{1/2}/(m\pi)^{1/2}$. In the region near the onset of convection, a convecting flow velocity is shown to grow as $\varepsilon^{1/2}$ from the perturbation theory for the hydrodynamic equations [41]. In Fig. 2 a fit of $\varepsilon^{1/2}$ to the MD data is also shown. The fitting coefficient of $\varepsilon^{1/2}$ is chosen to be 0.1 in Fig. 2. The microscopic MD results are found to agree well with the macroscopic hydrodynamic theory. In Fig. 2 the maximum flow velocity is not zero in the heat conduction state ($\varepsilon<0$). The MD data in this region show almost the same velocity and do not depend on the parameter ε. These nonzero velocities are thus due to the statistical simulation conditions such as the number of atoms and samplings.

The midelevation temperatures in the steady states are shown in Fig. 3 as a function of ε. The temperatures near the sidewall and at the center of the simulation region are almost the same as the average temperature when the Rayleigh number is smaller than the critical value ($\varepsilon<0$). It is thus found that the isothermal contours are parallel to the top and bottom walls and the heat conduction state is established in the system. It is noted that the distribution of the data is relatively large for $\varepsilon<0$ since the temperatures are normalized

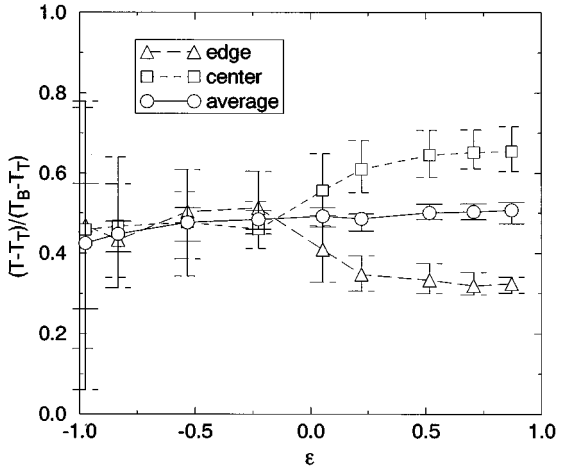

FIG. 3. Midelevation temperature in the steady state as a function of ε. The temperatures near the side wall (edge) and at the center (center) are shown along with the horizontal average (average).

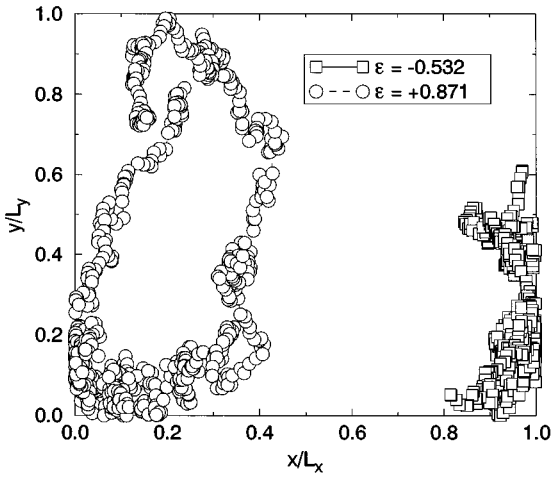

FIG. 4. Typical trajectories of atoms in the physical plane over 0.12×10^6 time steps (6000τ) in the steady state of the macroscopic flow field.

by the temperature difference between the top and bottom walls and the temperature difference is relatively small for $\varepsilon<0$. A bifurcation between conduction and convection is clearly seen at around the critical Rayleigh number ($\varepsilon=0$). When the Rayleigh number is larger than the critical value ($\varepsilon>0$), the isothermal contours are not parallel to the top and bottom walls and correspond to the velocity fields as shown in Fig. 1. A similar temperature bifurcation at around the critical Rayleigh number was shown using the DSMC method [6]. The MD method performed here is thus confirmed to qualitatively reproduce the conduction and convection states in the RB system.

IV. MICROSCOPIC MOTIONS OF ATOMS

In this section the relationship between the macroscopic flow phenomena and the microscopic motions of atoms are discussed. Typical trajectories of atoms in the physical plane are shown in Fig. 4, where positions of atoms are normalized by the height (L_y) and the width (L_x) of the simulation region. These trajectories are observed over 0.12×10^6 time steps (6000τ) in the steady state of the macroscopic flow field. It is shown, when the macroscopic flow field is convective ($\varepsilon=0.871$), that the atom is moving along the convection rolls. In the MD method, Eqs. (1)–(3) are deterministically solved and the macroscopic flow fields are obtained by sampling the microscopic motions of atoms. The trajectories of atoms are thus along the macroscopic flows. When the flow field is conductive ($\varepsilon=-0.532$), on the other hand, the trajectory seems to be random even if it may move along small-scale local flows.

A randomness of the motion of atoms is measured in terms of the growth rate of a separation distance between two trajectories in the phase space [42], which is composed of the position and the momentum of N atoms. At a certain time step during the MD simulation, the position of a certain atom in the phase space is slightly shifted as the initial condition for the calculation of the growth rate. The MD simulations for the shifted and the original systems are then performed. The separation distance is defined by

$$d(t)=\left(\sum_{i=1}^{N}\sum_{j=1}^{2}\{[p'_{i,j}(t)-p_{i,j}(t)]^2+[q'_{i,j}(t)-q_{i,j}(t)]^2\}\right)^{1/2}, \tag{8}$$

where p and q denote the momentum and the position of the atom in the original system, respectively, and p' and q' are those in the shifted system. The subscript j indicates the direction in the physical plane. After a certain time period Δt, the growth rate of the separation distance is obtained by $d(\Delta t)/d(0)$. A typical growth rate is shown in Fig. 5 as a function of Δt. The value of ε is 0.053 in this case. It is shown in Fig. 5 that the growth rate increases exponentially with time. The separation distance in the phase space is

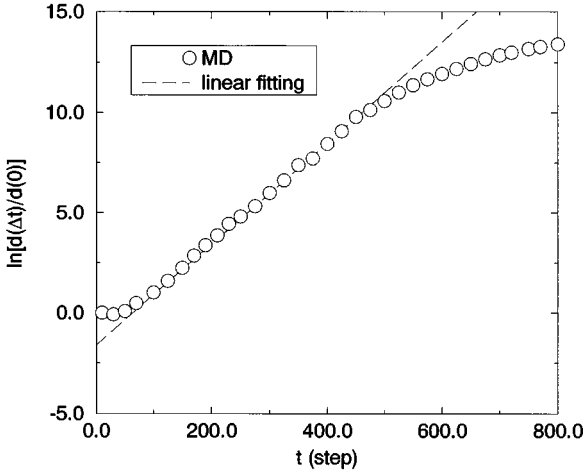

FIG. 5. Typical growth rate of the separation distance between two trajectories in the phase space for $\varepsilon=0.053$. A linear fit is also shown.

known to separate exponentially when the system is in a stochastic condition [42]. A chaotic motion of atoms is thus indicated in Fig. 5.

The chaotic motions of atoms are measured in terms of the Lyapunov exponent [41]. In our system, the Lyapunov exponent is defined by

$$\lambda = \lim_{n\to\infty} \frac{1}{n\Delta t} \sum_{k=0}^{n} \ln \frac{d_k(\Delta t)}{d_k(0)}, \tag{9}$$

where n denotes the number of samplings. The procedure for obtaining the growth rate is repeated until the Lyapunov exponent defined by Eq. (9) is sufficiently converged. This is an approximation of a more accurate method for the calculation of the Lyapunov exponents [33,34]. The time period is set equal to 200 time steps for all cases in our simulation.

The Lyapunov exponent is obtained from the growth rate of the separation distance as given by Eq. (9). We assume that the growth rate is dominated by the average relative speed of atoms in the physical space. As the average relative speed of atoms is proportional to the average speed of atoms in an equilibrium state, the growth rate in our system is assumed to be given by

$$\frac{d_k(\Delta t)}{d_k(0)} \propto \overline{v}, \tag{10}$$

where $\overline{v}$ is the average speed of atoms in the system. The average speed of atoms in the system, on the long-time average, is expressed as the sum of the average thermal speed for the average temperature in the system, the speed induced by gravity, and the speed due to macroscopic convection. The average thermal speed for the average temperature in the system is unity in the nondimensional form. The speed induced by gravity is proportional to $\Delta T/(T^*)^{1/2}$, since the gravitational acceleration is proportional to ΔT as given by Eq. (4) in our simulation and the reference velocity is proportional to $(T^*)^{1/2}$. The atomic speed due to macroscopic convection is proportional to $\varepsilon^{1/2}$ for $\varepsilon > 0$ as shown in Fig. 2. The average speed of atoms is thus given by

$$\overline{v} \propto 1 + a\frac{\Delta T}{(T^*)^{1/2}} + b\varepsilon 1/2, \tag{11}$$

where a and b are constants. The first and second terms on the right-hand side of the above relation indicate the effect of conduction in the macroscopic flow field, while the third term indicates that of macroscopic convection. The Lyapunov exponent is expressed by

$$\lambda = \ln\left(1 + a\frac{\Delta T}{(T^*)^{1/2}} + b\varepsilon^{1/2}\right) + c, \tag{12}$$

where c is a constant.

The Lyapunov exponents are shown in Fig. 6 as a function of ε. In Fig. 6 the Lyapunov exponents obtained by the MD simulation using Eqs. (8) and (9) are shown along with those obtained by a fit of Eq. (12) to the MD data. Equation (12) has three constants, each of which corresponds to a different thermodynamic state of the system: heat conduction, convection, and equilibrium. In Eq. (12), the constant

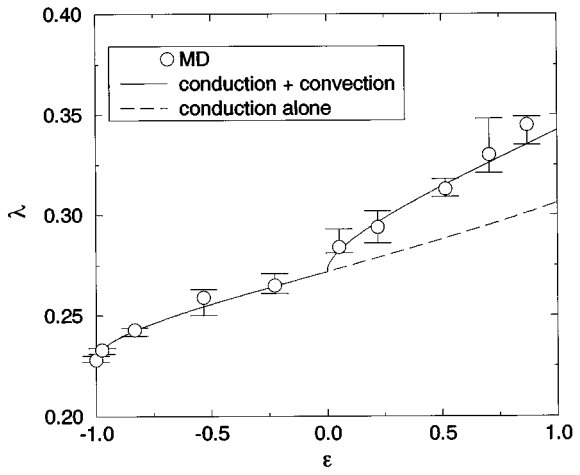

FIG. 6. Lyapunov exponents as a function of ε. A fit of Eq. (12) is also shown.

c is determined first as 0.228 from the MD data at $\varepsilon = -1$, where the system is in the equilibrium state with $\Delta T = 0$. The constant c depends on the simulation conditions such as the number of atoms and samplings. The constant a is then determined as 0.003 so as to obtain the good agreement between Eq. (12) and the MD data in the heat conduction state $(-1 < \varepsilon < 0)$. The magnitude of the speed induced by gravity is the order of $g\Delta t$, where g is given by Eq. (4) and Δt is the time period for the calculation of the Lyapunov exponent. This term is estimated to be about $0.001\Delta T/(T^*)^{1/2}$ from the simulation condition and thus the order of magnitude of the constant a is found to be in a reasonable range. The last constant b is determined as 0.04 so as to obtain the good agreement between Eq. (12) and the MD data in the convection state $(\varepsilon > 0)$. The coefficient of $\varepsilon^{1/2}$ in Fig. 2 is 0.1 and the order of magnitude of the constant b is also found to be in a reasonable range.

The effect of conduction, which is calculated from the first and second terms in the large parentheses of Eq. (12), is shown in Fig. 6 by the broken line, while the solid line is obtained using all the terms. It is shown in Fig. 6 that the Lyapunov exponent is well represented by the conduction part in Eq. (12) when the macroscopic flow field is conductive $(\varepsilon < 0)$. The conduction part, however, is not sufficient for the Lyapunov exponent when the macroscopic flow field is convection $(\varepsilon > 0)$. It is known, when the self-organized motion called dissipative structure is developed in the macroscopic flow field, that a part of the thermal energy is changed into kinetic energy [43]. The increase in kinetic energy in the macroscopic flow field corresponds to the increase in microscopic motions of atoms. The chaotic motions of atoms are thus found to increase when the macroscopic flow field is convective, which is a large-scale self-organized ordered motion of atoms. Although there may be other fittings to the MD data shown in Fig. 6, the agreement between the MD simulation and Eq. (12) is fairly good. Our assumption for the growth rate and the Lyapunov exponent is thus found to be appropriate.

V. SUMMARY

In this study we have simulated the macroscopic flow transition between heat conduction and convection in the RB

system using the MD method, which is a microscopic simulation technique. By changing the temperature difference between the top and bottom walls, we could simulate the macroscopic hydrodynamic phenomena in the RB system from heat conduction to convection. The large-scale flow was not observed and the motions of atoms were random in the heat conduction state, while the large-scale self-organized motion of atoms appeared in the convection state. In order to study the relationship between the macroscopic flow fields and the microscopic motions of atoms, the degree of the chaotic motions of atoms was observed in terms of the Lyapunov exponent, which was obtained from the growth rate of the separation distance between two trajectories in the phase space. The Lyapunov exponent was shown to increase with the average temperature and the temperature difference when the macroscopic flow field was conduction. It was found that the Lyapunov exponent was increased depending not only on the temperatures but also on the macroscopic flow velocity in the convection state. The chaotic motions of atoms were shown to increase in the large-scale self-organized ordered motion of atoms. It is of great concern whether the ordered motion results in the randomness of the microscopic motions or the increase in the chaotic motions of atoms results in the self-organized ordered motion. Our results demonstrate that the microscopic motions of atoms play an important role in a macroscopic flow transition or instability and the MD method is shown to be a valuable tool for studying the microscopic origin of macroscopic flow phenomena.

ACKNOWLEDGMENTS

The authors wish to thank Professor W. G. Hoover for useful comments and suggestions and Professor H. A. Posch for informing them of his recent works.

[1] G. Ahlers, Physica D **51**, 421 (1991).
[2] M. C. Cross and P. C. Hohenberg, Rev. Mod. Phys. **65**, 851 (1993).
[3] A. L. Garcia, in *Microscopic Simulations of Complex Flows*, edited by M. Mareschal (Plenum, New York, 1990), p. 177.
[4] S. Stefanov and C. Cercignani, Eur. J. Mech. B **11**, 543 (1992).
[5] A. Garcia and C. Penland, J. Stat. Phys. **64**, 1121 (1991).
[6] T. Watanabe, H. Kaburaki, and M. Yokokawa, Phys. Rev. E **49**, 4060 (1994).
[7] T. Watanabe, H. Kaburaki, M. Machida, and M. Yokokawa, Phys. Rev. E **52**, 1601 (1995).
[8] G. A. Bird, *Molecular Gas Dynamics and the Direct Simulation of Gas Flows* (Clarendon, Oxford, 1994).
[9] M. Mareschal and E. Kestemont, J. Stat. Phys. **48**, 1187 (1987).
[10] M. Mareschal and E. Kestemont, Nature **239**, 427 (1987).
[11] D. C. Rapaport, Phys. Rev. Lett. **60**, 2480 (1988).
[12] M. Mareschal, M. M. Mansour, A. Puhl, and E. Kestemont, Phys. Rev. Lett. **61**, 2550 (1988).
[13] A. Puhl, M. M. Mansour, and M. Mareschal, Phys. Rev. A **40**, 1999 (1989).
[14] J. A. Given and E. Clementi, J. Chem. Phys. **90** (12), 7376 (1989).
[15] H. A. Posch, W. G. Hoover, and O. Kum, Phys. Rev. E **52**, 1711 (1995).
[16] O. Kum, W. G. Hoover, and H. A. Posch, Phys. Rev. E **52**, 4899 (1995).
[17] W. G. Hoover and O. Kum, Mol. Phys. **86**, 685 (1995).
[18] E. Meiburg, Phys. Fluids **29**, 3107 (1986).
[19] D. C. Rapaport and E. Clementi, Phys. Rev. Lett. **57**, 695 (1986).
[20] D. C. Rapaport, Phys. Rev. A **36**, 3288 (1987).
[21] L. Hannon, G. C. Lie, and E. Clementi, Phys. Lett. A **119**, 174 (1986).
[22] B. L. Holian, Phys. Rev. A **37**, 2562 (1988).
[23] D. K. Bhattacharya and G. C. Lie, Phys. Rev. Lett. **62**, 897 (1989).
[24] D. K. Bhattacharya and G. C. Lie, Phys. Rev. A **43**, 761 (1991).
[25] D. L. Morris, L. Hannon, and A. L. Garcia, Phys. Rev. A **46**, 5279 (1992).
[26] J. Koplik, J. R. Banavar, and J. F. Willemsen, Phys. Rev. Lett. **60**, 1282 (1988).
[27] J. Koplik, J. R. Banavar, and J. F. Willemsen, Phys. Fluids A **1**, 781 (1989).
[28] J. Koplik and J. R. Banavar, Phys. Fluids A **5**, 521 (1993).
[29] J. Koplik and J. R. Banavar, Phys. Fluids **6**, 480 (1994).
[30] D. J. Evans, J. Chem. Phys. **78**, 3297 (1983).
[31] B. L. Holian, W. G. Hoover, and H. A. Posch, Phys. Rev. Lett. **59**, 10 (1987).
[32] W. G. Hoover, Phys. Rev. A **37**, 252 (1988).
[33] H. A. Posch and W. G. Hoover, Phys. Rev. A **38**, 473 (1988).
[34] H. A. Posch and W. G. Hoover, Phys. Rev. A **39**, 2175 (1989).
[35] W. G. Hoover and H. A. Posch, Phys. Rev. E **49**, 1913 (1994).
[36] W. G. Hoover and H. A. Posch, Phys. Rev. E **51**, 273 (1995).
[37] S. Chandrasekhar, *Hydrodynamic and Hydromagnetic Stability* (Clarendon, Oxford, 1961).
[38] L. Verlet, Phys. Rev. **159**, 98 (1967).
[39] S. Chapman and T. G. Cowling, *The Mathematical Theory of Non-Uniform Gases* (Cambridge University Press, Cambridge, 1970).
[40] D. M. Gass, J. Chem, Phys. **54**, 898 (1971).
[41] J. K. Bhattacharjee, *Convection and Chaos in Fluids* (World Scientific, Singapore, 1987).
[42] G. Casati and J. Ford, Phys. Rev. A **12**, 1702 (1975).
[43] P. Glansdorff and I. Prigogine, *Thermodynamic Theory and Structure, Stability and Fluctuations* (Wiley-Interscience, London, 1971).